

## PHOTODEFLECTION SPECTROSCOPY OF MAGNETOACTIVE SUPERLATTICES IRRADIATED BY BESSEL–GAUSSIAN LIGHT BEAMS\*

G. S. Mityurich,\*\* E. V. Chernenok, and A. N. Serdyukov

UDC 535.13

*The mechanism for the formation of photodeflection signals in magnetoactive superlattices irradiated by polarized modes of Bessel–Gaussian light beams is studied. The feasibility of controlling the spatial distribution of the temperature distribution in test samples with subsequent thermo-optical excitation of photodeflection signals is established. A method is proposed for nondestructive monitoring of the geometrical parameters of magnetoactive superlattices by means of laser photodeflection spectroscopy.*

**Keywords:** photodeflection spectroscopy, Bessel light beam, Maxwell equation, Green function, magnetoactive superlattice, Bessel function, heat transfer equation, photodeflection angle.

**Introduction.** Laser photodeflection spectroscopy is widely used in research on solids [1–3]. It is distinguished by its universality, high sensitivity, and relative ease of making measurements [4, 5]. In this paper, a photodeflection method is used to study short-period two-layer magnetoactive superlattices formed by cubic crystals of bismuth germanate ( $\text{Bi}_{12}\text{GeO}_{20}$ ) and bismuth silicate ( $\text{Bi}_{12}\text{SiO}_{20}$ ). Polarized *TE*- and *TH*-modes of Bessel-Gaussian light beams (BGLB) are used to excite thermoelastic oscillations in the samples [6, 7].

Laser photodeflection spectroscopy is based on the conversion of the energy absorbed from a light beam in the volume of a sample into a thermal field which produces a refractive index gradient in the sample and the surrounding medium. The deflection from the horizontal of a low-power probe laser beam as it passes through the region with a nonuniform refractive index yields information on the optical, dissipative, thermal, and other characteristics of the sample.

**Determination of the BGLB Energy Loss Rate and of the Deflection Angles.** Let an amplitude modulated Bessel light beam, e.g., with *TE*-polarization, be incident normally on a magnetically active superlattice (Fig. 1) consisting of cubic crystals such as bismuth germanate or bismuth silicate. In the long-wavelength approximation [8, 9] a two-layer superlattice can be represented as a single-layer crystal with its optical axis perpendicular to the boundary of the layers, since the beam is normally incident on the sample. A two-layer magnetoactive superlattice is characterized [10] by uniaxial complex dielectric  $\varepsilon_{ij}$  and induced optical activity  $G_{ij}$  tensors. The corresponding principal values of these effective tensors are given by

$$\varepsilon_{\text{eff}} = (\varepsilon_e)_{11} = (\varepsilon_e)_{22} = x_0\varepsilon_1 + (1 - x_0)\varepsilon_2, G_{\text{eff}} = (G_e)_{11} = (G_e)_{22} = x_0G_1 + (1 - x_0)G_2, \quad (1)$$

where  $x_0 = d_1/D$ , with  $D = d_1 + d_2$  being the superlattice period;  $d_1$  и  $d_2$  are the thicknesses of the superlattice components;  $\varepsilon_{1,2} = \varepsilon'_{1,2} + i\varepsilon''_{1,2}$  and  $G_{1,2} = G'_{1,2} + iG''_{1,2}$  are the complex dielectric constants and complex magnetic gyration parameters of the components of the magnetoactive superlattice, with the real part  $G'_{1,2}$  determining the specific rotation of the plane of polarization of the wave in the components of the structure and the imaginary part  $G''_{1,2}$  corresponding to the magnetic circular dichroism in layers  $d_1$  and  $d_2$ .

Based on the material equations for magnetoactive media [11, 12],

$$\mathbf{E} = \mathbf{G}^{-1}\mathbf{D}, \quad \mathbf{B} = \mu\mathbf{H}, \quad (2)$$

\* Presented at the international conference "Optics of Crystals," September 23–26, 2014, Mozyr, Belarus.

\*\* To whom correspondence should be addressed.

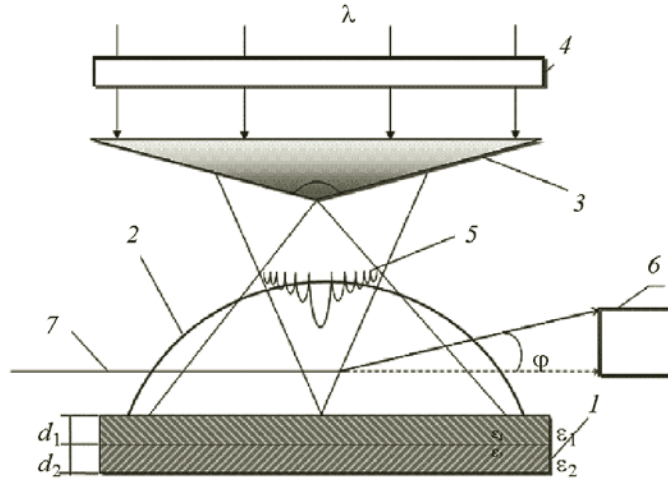


Fig. 1. Configuration for the detection of a photodeflection signal: (1) magnetoactive superlattice; (2) "thermal" lens; (3) axicon; (4) modulator; (5) *TE*-mode Bessel light beam; (6) position-sensitive photodetector; (7) probe beam.

where  $G^{-1} = (\varepsilon^{-1} + i\mathbf{G}^{\times})$ ,  $\mathbf{G}^{\times}$  is an antisymmetric complex second-rank tensor that is dual to the magnetic gyration vector  $\mathbf{G}$ , and  $\mu = 1$ , on the solutions of the Maxwell equations

$$\text{rot } \mathbf{E} = [\nabla \mathbf{E}] = ik_0 \mathbf{B}, \quad \text{rot } \mathbf{H} = [\nabla \mathbf{D}] = ik_0 \mathbf{D}, \quad (3)$$

in a cylindrical coordinate system ( $\nabla \mathbf{A} = (1/\rho)[\partial(\rho A_\rho)/\partial \rho] + (1/\rho)[\partial A_\phi/\partial \phi] + \partial A_z/\partial z$ ), and on Eqs. (1), we obtain an expression for the rate of dissipation of the energy of the *TE*-mode of a Bessel light beam in a two-layer magnetoactive superlattice,

$$Q^{TE} = Q_0^{TE} \exp(-\alpha_{\text{eff}} z). \quad (4)$$

Here  $Q_0^{TE} = \frac{\omega k_0^4 I_0}{8\pi} \left( \frac{m^2}{\rho^2} J_m^2(q\rho) + J_m'^2(q\rho) \right) |V_0| \|\varepsilon_{\text{eff}}\| \text{Re} \sqrt{\varepsilon_{\text{eff}}} \text{Im} \sqrt{\varepsilon_{\text{eff}}}$ , where  $\alpha_{\text{eff}} = 2k'_0(x_0\varepsilon_1'' + (1-x_0)\varepsilon_2'')^{1/2}$  is the effective absorption index for the superlattice;  $I_0$  is the intensity of the light beam;  $J_m(q\rho)$  is the first order Bessel function of order  $m$ ;  $J_m'(q\rho)$  is the derivative of the Bessel function with respect to the radial coordinate  $\rho$ ;  $k'_0 = k_0 \cos \alpha_0 = \alpha_0 \omega/c$ , where  $\alpha_0$  is the conicity of the Bessel light beam, which equals half the angle at the vertex of the cone of wave vectors that determine the spectrum of the spatial frequencies of the beam; and  $V_0 = \frac{\sqrt{x_0\varepsilon_1 + \varepsilon_2(1-x_0)}}{k_0'^2 - [G_1x_0 + G_2(1-x_0)]^{-1}k_0^2}$ . Equation (4) gives the power density of the thermal sources in the heat conduction equation that describes the temperature field in the sample.

The overall rate of dissipation for a BGLB [13] modulated at frequency  $\Omega$  can be written in the form

$$Q = Q^{TE} \exp(-2r^2/w_0^2)(1 + \cos \Omega t), \quad (5)$$

where  $r^2 = x^2 + y^2$  and  $w_0$  is the beam waist.

We consider the case of a transverse geometry for the interaction of the driver Bessel light beam and the probe beam (Fig. 1). Because of the modulated absorption of the light incident on the sample, a nonstationary temperature distribution develops in the sample; that distribution corresponds to the solution of the inhomogeneous differential equation

$$\nabla^2 T - \frac{1}{\beta_S} \frac{\partial T}{\partial t} = \frac{1}{2k_S} Q_0^{TE} \exp(-\alpha_{\text{eff}} z) \exp(-2r^2/w_0^2) (1 + \cos \Omega t), \quad (6)$$

where the thermal diffusivity  $\beta_S$  is related to the thermal conductivity by  $\beta_S = k_S/\rho_0 C$ ,  $\rho_0$  is the density, and  $C$  is the specific heat. We seek a solution of Eq. (6) of the form

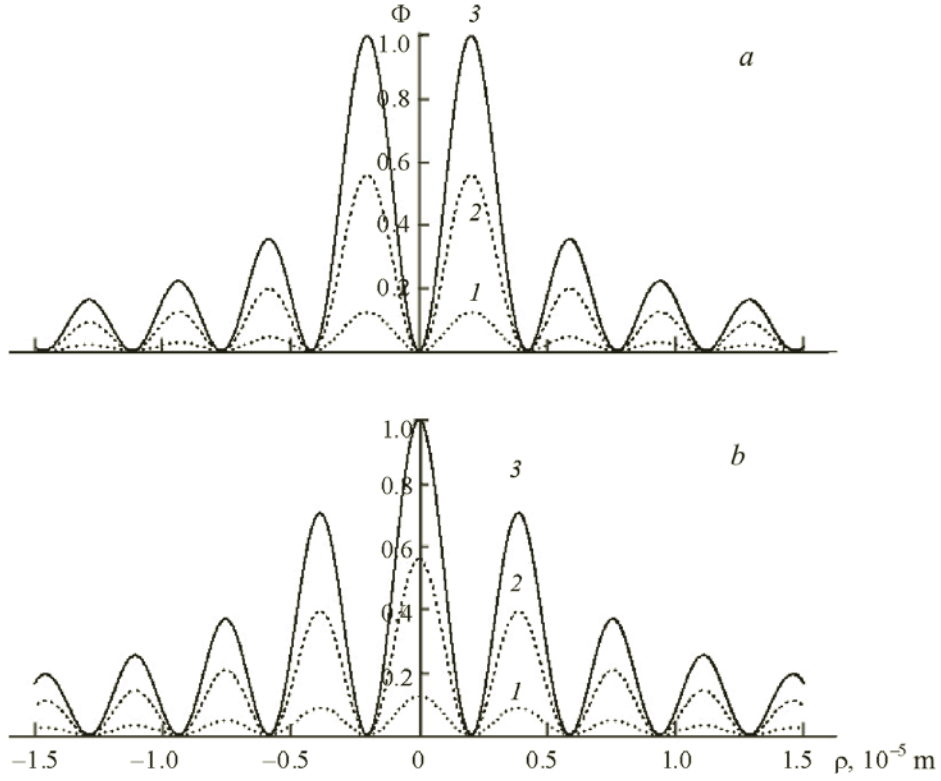


Fig. 2. Photodeflection angle as a function of radial coordinate  $\rho$  for  $TE$ -modes of the Bessel light beam:  $m = 0$  (a) and  $m = 1$  (b);  $t = 0.10$  (1),  $0.15$  (2), and  $0.20$  s (3).

$$T(x, y, z, t) = \int_{-\infty}^{+\infty} \int_{-\infty}^{+\infty} \int_0^{+\infty} \int_0^{+\infty} Q^{TE}(\xi, \eta, \mu, \chi) G(\xi, \eta, \mu, \chi) d\xi d\eta d\mu d\chi, \quad (7)$$

subject to the standard boundary conditions. In Eq. (7),  $G(\xi, \eta, \mu, \chi)$  is the Green function

$$G = \frac{\Theta(t)}{8\pi^{3/2} \rho C \beta_S (t - \tau)^{3/2}} \exp\left[-\frac{(x - \xi)^2}{4\beta_S (t - \tau)}\right] \exp\left[-\frac{(y - \eta)^2}{4\beta_S (t - \tau)}\right] \exp\left[-\frac{(z - \mu)^2}{4\beta_S (t - \tau)}\right], \quad (8)$$

that satisfies the operator equation

$$\Delta G - (1/\beta_S)(\partial G/\partial t) = -(2k_S)^{-1} \delta(x - \xi, y - \eta, z - \mu) \delta(t - \chi), \quad (9)$$

where  $\Theta(t)$  is the Heaviside unit step function and  $\delta(x - \xi, y - \eta, z - \mu)$  and  $\delta(t - \chi)$  are Dirac delta functions of the spatial and time coordinates.

Substituting Eq. (8) in Eqs. (5) and (7) and calculating the integrals over the spatial variables, it is easy to obtain the temperature distribution in a magnetoactive superlattice:

$$T(x, y, z, t) = Q_0^{TE} \exp(-\alpha_{\text{eff}} z) \int_0^t \frac{1 + \cos \Omega t}{w_0^2 + 8\beta_S (t - \tau)} \exp\left[-\frac{x^2 + y^2}{w_0^2 + 8\beta_S (t - \tau)}\right] \exp[-\alpha_{\text{eff}}^2 \beta_S (t - \tau)] d\tau. \quad (10)$$

The photodeflection angle for the probe beam for a transverse interaction geometry is determined [14] using the equation

$$\Phi = \frac{1}{n_{\text{eff}}} \frac{dn_{\text{eff}}}{dT} \int \frac{\partial T(x, y, z, t)}{\partial x} dy, \quad (11)$$

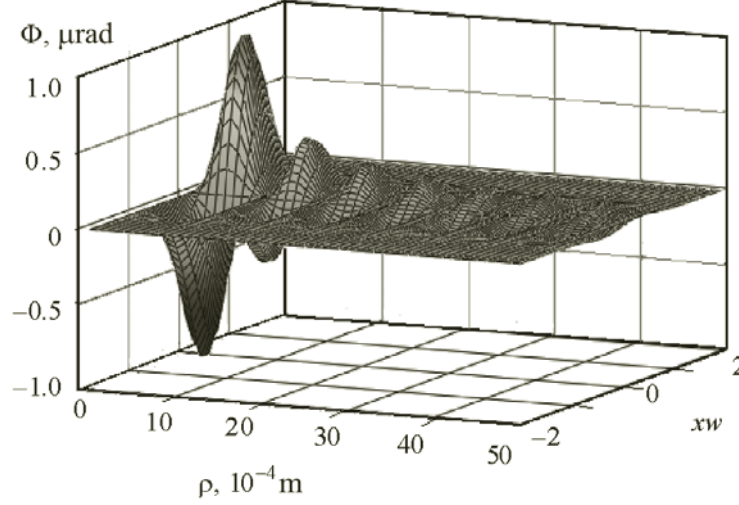


Fig. 3. Photodeflection angle  $\Phi$  as a function of radial coordinate  $\rho$  and the normalized coordinate  $xw = x/w_0$  ( $m = 0$ ).

where  $n_{\text{eff}} = \sqrt{\varepsilon_{\text{eff}}}$  is the unperturbed effective refractive index of the superlattice.

After substituting Eq. (10) in Eq. (11) and some further transformations, we obtain the desired expression for the photodeflection signal:

$$\Phi(\rho, z, t) = \frac{\omega k_0^4 I_0}{2n_{\text{eff}} \sqrt{\pi}} \frac{dn_{\text{eff}}}{dT} |V_0| |\varepsilon_{\text{eff}}| \text{Re} \sqrt{\varepsilon_{\text{eff}}} \text{Im} \sqrt{\varepsilon_{\text{eff}}} \left( \frac{m^2}{\rho^2} J_m^2(q\rho) + J_m'^2(q\rho) \right) \times \exp(-\alpha_{\text{eff}} z) \int_0^t \frac{(\sin^2 \Omega t - 1) x}{[w_0^2 + 8\beta_S(t - \tau)]^{3/2}} \exp\left[-\frac{x^2 + y^2}{w_0^2 + 8\beta_S(t - \tau)}\right] \exp[-\alpha_{\text{eff}}^2 \beta_S(t - \tau)] d\tau. \quad (12)$$

As Eqs. (10) and (11) show, the spatial distribution of the temperature and the amplitude of the photodeflection signal depend in complicated ways on the dissipative, geometrical, and thermal parameters of the superlattice and on the polarization properties of the quasi-diffractionless light beams. Thus, in the following, we use numerical integration to analyze the dependences of the temperature distribution and photodeflection angles on the parameters of the sample and the properties of the incident light.

**Results and Discussion.** In order to make the calculations of the photodeflection transformation in two-layered samples more specific, we choose values of the parameters and constants [15, 16] for the class 23 cubic magnetoactive crystals bismuth germanate ( $\text{Bi}_{12}\text{GeO}_{20}$ ) and bismuth silicate ( $\text{Bi}_{12}\text{SiO}_{20}$ ) of which the superlattice is made: light beam intensity  $I_0 = 0.15 \text{ W/cm}^2$ , beam waist  $w_0^2 = 0.5 \cdot 10^{-3} \text{ m}$ , thicknesses of the components in the sample  $d_1 = 80 \cdot 10^{-9} \text{ m}$  and  $d_2 = 120 \cdot 10^{-9} \text{ m}$ ,  $dn_{\text{eff}}/dT = 2.5 \cdot 10^{-6}$ ,  $\varepsilon_1 = 7 + i2 \cdot 10^{-2}$ ,  $\varepsilon_2 = 4 + i \cdot 10^{-2}$ ,  $G_1 = 10^{-4} + i2 \cdot 10^{-5}$ ,  $G_2 = 10^{-5} + i2 \cdot 10^{-6}$ ,  $\lambda = 5 \cdot 10^{-7} \text{ m}$ ,  $\beta_1 = 0.4 \cdot 10^{-4} \text{ m}^2/\text{s}$ ,  $\beta_2 = 0.74 \cdot 10^{-4} \text{ m}^2/\text{s}$ ,  $z = 200 \cdot 10^{-9} \text{ m}$ ,  $c = 3 \cdot 10^8 \text{ m/s}$ ,  $k_S = 100$ ,  $\beta_{S1} = 0.4 \cdot 10^{-4} \text{ m}^2/\text{s}$ , and  $\beta_{S2} = 0.74 \cdot 10^{-4} \text{ m}^2/\text{s}$ .

Figure 2 shows that the temperature distribution is a rapidly oscillating function of the radial coordinate  $\rho$ , with a temperature maximum or minimum at the center of the exciting beam ( $\rho = 0$ ) determined by the mode number of the Bessel light beam ( $m = 0$  in Fig. 2a and  $m = 1$  in Fig. 2b). As the time the laser source acts on the sample increases, the temperature rises and oscillates in phase for the different modes of the laser. For certain values of the radial coordinate, regions of maximum and minimum heat release appear. Thus, as opposed to the case of plane waves, the temperature distribution in the sample is determined by the intensity profile of the polarization modes of the Bessel light beam.

The way the energy of the Bessel light beam is dissipated, the ratio of the thicknesses of the components of the sample, and the modulation frequency of the incident light beam all have a significant influence on the formation of the photodeflection response from a magnetoactive superlattice. Figure 3 shows how the amplitude of the photodeflection signal

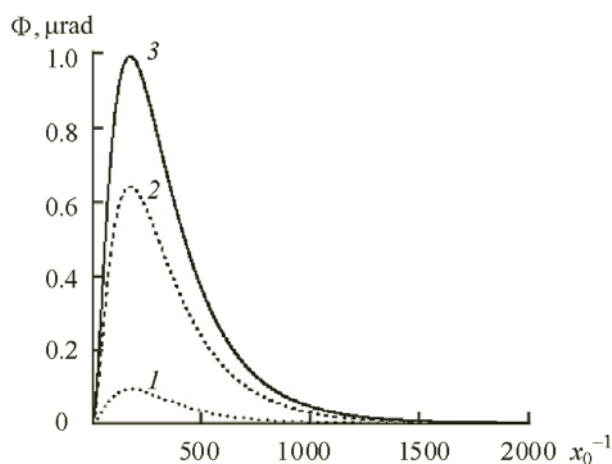


Fig. 4. Photodeflection angle as a function of the relative superlattice thickness  $x_0 = d_1/D$ ;  $m = 0$ ;  $t = 0.05$  (1), 0.10 (2), and 0.15 s (3).

is symmetric with respect to changes in the normalized coordinate ( $x/w_0$ ) and falls off exponentially, while oscillating, as a function of the radial coordinate  $\rho$ ; this correlates with the temperature distribution and is related to the modulating effect of the Bessel function. As the modulation frequency of the beam that drives the photodeflection response is raised, the amplitude of the oscillations falls off exponentially owing to the thermal inertia of the light-to-heat conversion process.

The dependence of the photodeflection angles on the relative superlattice thickness  $x_0 = d_1/D$  (Fig. 4) contains maxima with amplitudes that grow as the irradiation time increases ( $t = 0.05, 0.10$ , and  $0.15$  s). Experimental measurement of the photodeflection response corresponding to the peaks in the  $\Phi = f(x_0^{-1})$  curves can be used to determine the relative thickness  $x_{0\max}$  of a two-layer sample for which the absorptivity of the superlattice will reach a maximum.

The photodeflection signal also depends on the conicity angle of the axicon for different modes of the Bessel light beam and, correspondingly, affects the temperature distribution in the sample [17]. Different ways have been developed [18–22] for adjusting the conicity angle with a short time for changing the angular spectrum of the modes of the Bessel light beam. Fast electro-optical schemes for varying the spatial intensity distribution of the light field with conicity are described elsewhere [23, 24]. A device has been proposed [25] for thermo-optical excitation of acoustic waves based on choosing the necessary modes for quasi-diffractionless light beams. Thus, further development of methods for controlling photoacoustic and photodeflection conversion using Bessel light beams appears to be most promising for nondestructive monitoring and diagnostics of nonuniform materials and of thin-film and low-dimensionality structures.

**Conclusions.** A study by laser photodeflection spectroscopy of the properties of magnetoactive superlattices irradiated by different modes of Bessel light beams demonstrates the feasibility of controlling the temperature distribution in a sample with subsequent excitation of photodeflection signals by formation of the required polarization modes of Bessel–Gaussian beams. This is done by using axicons with variable conicity or using optical schemes with varying conicity of Bessel light beams. These results indicate that the measured amplitude of the photodeflection signal can be used as a method for nondestructive monitoring of the geometrical parameters of magnetoactive superlattices during their fabrication.

This work was supported by the Foundation for Basic Research of the Republic of Belarus (grant No. F14-047).

## REFERENCES

1. W. B. Jackson, N. M. Amer, A. C. Boccara, and D. Fournier, *Appl. Opt.*, **20** (6), 1333–1344 (1981).
2. A. Mandelis, *Principles and Perspectives of Photothermal and Photoacoustic Phenomena*, Elsevier, New York (1992).
3. V. P. Zharov and V. S. Letokhov, *Laser Opto-Acoustic Spectroscopy* [in Russian], Nauka, Moscow (1984).
4. A. Yu. Luk'yanov, V. G. Ral'chenko, A. V. Khomich, A. V. Serdtsev, P. V. Volkov, A. V. Savel'ev, and V. I. Konov, *Kvant. Elektron.*, **38** (12), 1171–1178 (2008).
5. S. E. Bialkowski, *Photothermal Spectroscopy Methods for Chemical Analysis*, Wiley-Interscience (1996).
6. J. Durnin, *J. Opt. Soc. Am.*, **4** (4), 651–654 (1987).
7. A. N. Pyatnitskii, *Bessel Wave Fields* [in Russian], Fizmatlit, Moscow (2012).

8. S. M. Rytov, *Zh. Eksp. Teor. Fiz.*, **29** (5), 605–616 (1955).
9. L. Brillouin and M. Parodi, *Wave Propagation in Periodic Structures* [Russian translation], Mir, Moscow (1959).
10. V. E. Gaishun, I. V. Semchenko, and A. N. Serdyukov, *Kristallografiya*, **38** (3), 24–27 (1993).
11. F. I. Fedorov, *Theory of Gyrotropy* [in Russian], Nauka i Tekhnika, Minsk (1976).
12. S. S. Girgel', *Basic Theoretical Crystal-Optics of Magnetically-Ordered Media* [in Russian], Gomel (2008).
13. D. N. Schimpf, W. P. Putnam, M. D. W. Grogan, S. Ramachandran, and F. X. Kärtner, *Opt. Express*, **21** (15), 18483–18496 (2013).
14. G. S. Mintyurich and P. V. Astakhov, *Zh. Tekh. Fiz.*, **64** (12), 2–8 (1994).
15. A. A. Blistanov, V. S. Bondarenko, N. V. Perelomov, and N. P. Shaskol'skaya (Eds.), *Acoustic Crystals. A Handbook* [in Russian], Nauka, Moscow (1982).
16. I. S. Grigor'ev and E. Z. Meilikhov (Eds.), *Physical Quantities. A Handbook* [in Russian], Energoatomizdat, Moscow (1991).
17. G. S. Mintyurich, E. V. Chernenok, V. V. Sviridova, and A. N. Serdyukov, *Problemy Fiziki, Matematiki i Tekhniki*, **21**, No. 4 (2014).
18. V. Vaicaitic and S. Paulicas, *Opt. Quantum Electron.*, **35**, 1065–1071 (2003).
19. S. Klewitz, F. Brinkmann, S. Herminghaus, and P. Leiderer, *Appl. Opt.*, **34**, 7670–7675 (1995).
20. R. Borghi and M. Santarsiero, *J. Opt. Soc. Am.*, **44** (1), 23–26 (1997).
21. A. Dubietis, P. Polesana, G. Valiulis, A. Stabinis, P. Di Trapani, and A. Piskarskas, *Opt. Express*, **15** (7), 4168–4175 (2007).
22. S. Akturk, *Opt. Comm.*, **282** (16), 3206–3209 (2009).
23. N. S. Kazak, M. Krening, A. G. Mashchenko, and P. I. Ropot, *Opt. Spektrosk.*, **103** (5), 826–830 (2007); *Opt. Spectrosk.*, **103** (5), 816–830 (2007).
24. S. V. Solonevich, A. A. Ryzhkevich, N. S. Kazak, M. K. Al-Mukhanna, S. Kh. Al-Hovaiter, and T. S. M. Al-Saud, *Proc. 9th Int. Conf. "Interaction of Radiation with Solids,"* September 20–22, 2011, Minsk (2011), pp. 451–452.
25. P. I. Ropot and G. S. Mintyurich, *Apparatus for Thermo-Optical Excitation of Acoustic Waves*, Patent No. 5969, Republic of Belarus (2010).

Copyright of Journal of Applied Spectroscopy is the property of Springer Science & Business Media B.V. and its content may not be copied or emailed to multiple sites or posted to a listserv without the copyright holder's express written permission. However, users may print, download, or email articles for individual use.